

Quantification of antagonistic optomechanical forces in an interferometric detection system for dynamic force microscopy

L. Tröger and M. Reichling^{a)}

Fachbereich Physik, Universität Osnabrück, Barbarastr. 7, 49076 Osnabrück, Germany

(Received 2 March 2010; accepted 12 October 2010; published online 24 November 2010)

In fiber-optic interferometer systems detecting oscillatory cantilever motion, the intensity distribution of the light field in the interferometric cavity generates an optomechanical coupling determining the effective properties of the oscillating system. For a low finesse cavity established by an uncoated cantilever and the fiber end, the resonance frequency and spring constant are shifted mainly due to radiation pressure whereas the Q -factor is varied due to photothermal forces under typical conditions. We find, that radiation pressure and photothermal force act in opposite directions and discuss the retardation times governing the antagonistic effects differing by orders of magnitude. © 2010 American Institute of Physics. [doi:10.1063/1.3509412]

Laser-interferometry is a means of precisely measuring distances with applications ranging from gravitation wave detectors¹ to subnanometer oscillation detection in scanning probe microscopy.² In the context of the interferometric detection systems³ of a noncontact atomic force microscope⁴ (NC-AFM), the impact of cross coupling between optical and mechanical parts^{5–8} on the experimental performance has been discussed mainly for coated cantilevers where the direction and size of photothermal forces depends on unknown subtleties of the coating.^{5,8–10} We investigate the interaction of the light field with uncoated cantilevers in the interferometric detection system of a NC-AFM and quantify the antagonistic forces due to radiation pressure and photothermal deflection.

We use a home-built NC-AFM inspired by the system presented in Ref. 11 operated in ultrahigh vacuum (UHV) with an interferometric detection system utilizing an uncoated monomode glass fiber with a nylon cladding cut with an ultrasonically driven diamond blade (FK11, Photon Kinetics, Beaverton, USA). Experiments are performed at room-temperature using an uncoated silicon cantilever (Pointprobe FM, Nanoworld, Neuchâtel, Switzerland) with a mechanical spring constant calculated from its dimensions and resonance frequency¹² to be $k_{\text{mech}}=1.3 \text{ N m}^{-1}$. The cantilever is covered by a native oxide. However, the effect of the oxide layer is negligible for our study as it has a thickness of typically 2 nm only,¹³ it does not absorb light and its thermomechanical properties do not differ strongly from those of silicon.¹⁴ We examine the influence of the radiation field within the cavity formed by the cantilever backside and the cleaved fiber end face on the oscillation properties of the cantilever in dependence of the cavity length D . The intensity distribution of the light field in the cavity and the resulting radiation force gradient are shown in Fig. 1(a). The most sensitive points for interferometric detection of positive and negative slopes are marked in Fig. 1(a) by numbered circles. At these points, resonance spectra of the thermally excited cantilever are taken and plotted in Fig. 1(b). Starting from contact between the fiber end and the cantilever, the cantilever is retracted along an axis z by its supporting piezo tube over four interference minima covering a distance of $1.6 \mu\text{m}$ for the wavelength of $\lambda=780 \text{ nm}$. Resonance frequencies and Q -factors

for spectra taken at cavity length values $D_n(n=1, 2, \dots, 8)$ corresponding to maximum slope positions are evaluated by fitting a theoretical curve to the experimental data.¹⁵ Results are compiled in Table I.

Spectra 1 and 2 are not considered for further analysis as they are shifted by nearly 2 Hz presumably due to electrostatic interactions between the fiber and the cantilever. The other spectra shown in Fig. 1(b) taken at positions of positive

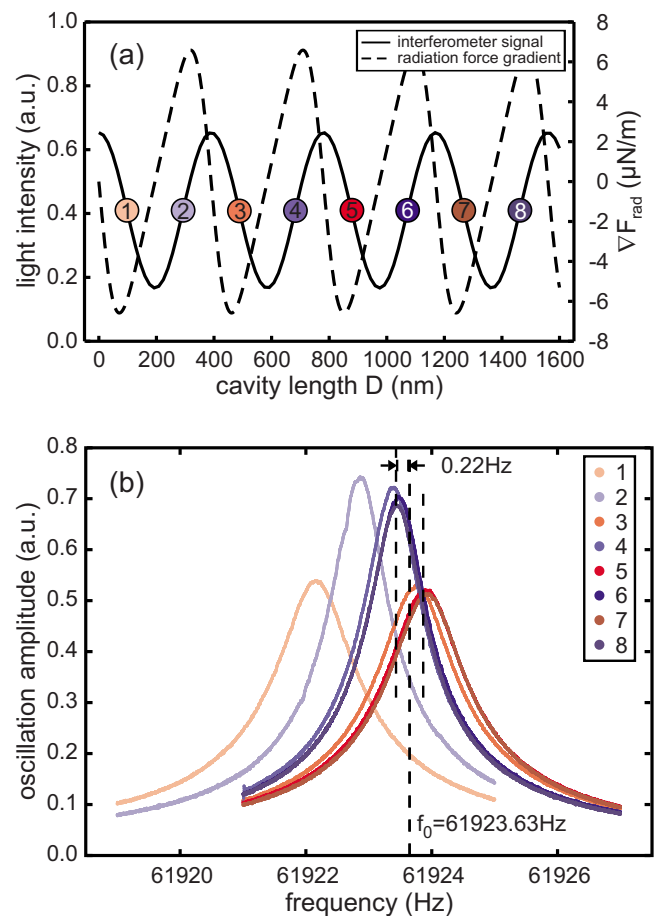


FIG. 1. (Color online) (a) Progression of the interferometric intensity and optical force gradient due to radiation pressure as a function of cavity length. (b) Resonance curves of the thermally excited cantilever taken at positions 1, 3, 5, and 7 for negative slope and positions 2, 4, 6, and 8 for positive slope marked in frame (a).

^{a)}Electronic mail: reichling@uos.de.

TABLE I. Effective values for the resonance frequency $\omega_{\pm}/2\pi$ and quality factor $Q^{\pm}=\omega_0/\Gamma^{\pm}$ (Γ : damping constant) determined from resonance curves taken at the most sensitive points of the alternating slopes of the interferometric signal. Positions n correspond to the numbering in Fig. 1. Subscripts and superscripts \pm denote positive or negative slopes.

Position n	Slope	$\omega_{\pm}/2\pi$ (Hz)	Q^{\pm}	Γ^{\pm} (1/s)
1	Negative	61 922.15	52 200	7.45
2	Positive	61 922.85	73 900	5.26
3	Negative	61 923.75	53 900	7.22
4	Positive	61 923.38	73 300	5.31
5	Negative	61 923.89	53 400	7.29
6	Positive	61 923.46	72 900	5.34
7	Negative	61 923.92	53 100	7.33
8	Positive	61 923.44	72 400	5.37

or negative slope, respectively, differ in both, their resonance frequency that is shifted from the eigenfrequency ω_0 to ω_{\pm} as well as the effective Q -values due to the coupling between mechanical and optical springs (see Table I). The subscript and superscript \pm refer to the interferometer positions of maximum positive and negative slopes, respectively.

$$\frac{k^{\pm}}{k_{mech}} = \frac{\omega_{\pm}^2}{\omega_0^2} = 1 - \underbrace{\frac{1}{1 + \omega_0^2 \tau_{pt}^2} \frac{\nabla F_{pt}^{\pm}}{k_{mech}}}_{\varphi_{pt}^{\pm}} - \underbrace{\frac{1}{1 + \omega_0^2 \tau_{rad}^2} \frac{\nabla F_{rad}^{\pm}}{k_{mech}}}_{\varphi_{rad}^{\pm}} \quad (1)$$

$$\frac{\Gamma^{\pm}}{\Gamma_0} = 1 + Q_0 \left(\frac{\omega_0 \tau_{pt}}{1 + \omega_0^2 \tau_{pt}^2} \frac{\nabla F_{pt}^{\pm}}{k_{mech}} + \frac{\omega_0 \tau_{rad}}{1 + \omega_0^2 \tau_{rad}^2} \frac{\nabla F_{rad}^{\pm}}{k_{mech}} \right). \quad (2)$$

Equations (1) and (2) are valid for oscillation frequencies in a narrow range around the eigenfrequency ω_0 of the cantilever. As evident from Eq. (1), the quantities φ_{pt}^{\pm} and φ_{rad}^{\pm} can be interpreted as contributions of the photothermal effect and the photon pressure to the effective force constant k^{\pm} normalized to the mechanical force constant k_{mech} . Thus they describe the relative weight of the respective optomechanical effect.

The force originating from the radiation pressure is fully defined by the properties of the optical cavity and the force gradient can be described as the rigidity of an optical spring $k_{rad} = -\partial F_{rad} / \partial D$. Note, that k_{rad} periodically varies from positive to negative values and back when increasing the cavity length. While the maximum optical resonance is obtained for cavity length values $D = n/2 \cdot \lambda$, $n \in \mathbb{N}$, maximum detection sensitivity for a cavity with a low finesse⁹ (in our case $\mathcal{F} = 1.2$) is yielded for detuning the cavity to^{16,17}

$$D_n^{\pm} = \left\{ \begin{array}{l} D_n^+ \forall n = 2k \\ D_n^- \forall n = 2k - 1 \end{array} \right\} = \left(\frac{2n+1}{8} \right) \cdot \lambda; k, n \in \mathbb{N} \quad (3)$$

As shown in Ref. 18 and illustrated in Fig. 1, this yields a positive force gradient for $D = D_n^+$ and a negative force gradient for $D = D_n^-$, namely:

Due to the symmetry of the interferometric signal it can be assumed that the eigenfrequency of the cantilever is the arithmetic mean of the shifted values, namely, $f_0 = \omega_0/2\pi = 61\,923.63$ Hz, and the light induced shift in the resonance frequency is ± 0.22 Hz. The intrinsic quality factor $Q_0 = 61\,675.1$ of the oscillation is calculated from the measured values as described in Ref. 8. Notably we find, that on the negative slope, the minute positive shift in resonance frequency comes along with a 15% reduction in the Q -factor and vice versa for measurements on the positive slope.

To quantitatively interpret the experimental data, we adopt a model describing the optomechanical interactions by photothermal and radiation forces F_{pt} and F_{rad} acting on the cantilever in the light field of the cavity.⁵ The cross-coupling of optical and mechanical properties determines the effective spring constants k^{\pm} , resonance frequencies ω_{\pm} , and damping factors $\Gamma^{\pm} = \omega_0/Q^{\pm}$ at the maximum slope positions. The shift in the oscillation parameters critically depends on retardation times τ_{pt} and τ_{rad} governing the interaction between the optical and mechanical resonator and the optical force gradients ∇F_{pt} and ∇F_{rad} generated by the interferometer light intensity distribution at the cantilever position¹⁰ and can be described as follows:

$$\nabla F_{rad}(D) = \frac{d}{dD} \left[\frac{(2R_2 + A_2)T_1 P}{|1 - \sqrt{R_1 R_2} e^{-i(4\pi D/\lambda)}|^2} c \right],$$

$$\nabla F_{rad}(D_n^{\pm}) = \nabla F_{rad}^{\pm} = \pm 11.4 \mu\text{N m}^{-1}. \quad (4)$$

With the transmittance of the incoming laser light (power $P = 960 \mu\text{W}$) into the cavity being $T_1 = 96\%$. The reflectivity of the fiber end face is $R_1 = 3.5\%$ and we assume $R_2 = 37\%$ for the cantilever back side^{19,20} and $A_2 = 0.3$ for the fraction of light absorbed by the cantilever¹⁴ while c denotes the speed of light.

To quantify the optomechanical retardation effect, we first consider the retardation time for the radiation force that is equal to the storage time of photons in the optical cavity²¹ and find it to be of the order of $\tau_{rad} = 2\mathcal{F}D_1^-/\pi c = 0.01$ ps. Combining this with the result from Eq. (4), we find $\varphi_{rad}^{\pm} = \pm 8.7 \times 10^{-6}$ and can further use Eq. (1) to calculate the contribution of the detuning due to the photothermal force φ_{pt}^{\pm} based on the experimental data from Table I as follows:

$$\varphi_{\text{pt}}^{\pm} = 1 - \frac{\omega_{\pm}^2}{\omega_0^2} - \varphi_{\text{rad}}^{\pm} = \mp 1.55 \times 10^{-6}. \quad (5)$$

This reveals that the small shift in resonance frequency is mainly due to the radiation force acting on the oscillating cantilever but reduced by approximately 18% due to the counter acting force of photothermal effects.

The photothermal time constant τ_{pt} is determined by material properties and the geometry of the cantilever.²² It can be derived from the experimental data of the Q -factor change exploiting Eq. (2). Neglecting the contribution of the radiation pressure as $\omega_0\tau_{\text{rad}} = 6.5 \times 10^{-9} \ll 1$, we find:

$$\tau_{\text{pt}} = \left(\frac{\Gamma^{\pm}}{\Gamma} - 1 \right) \frac{1}{Q_0\omega_0\varphi_{\text{pt}}^{\pm}} = 4.1 \text{ } \mu\text{s}. \quad (6)$$

This reveals a significant change in the Q -factor with a normalized contribution of $Q_0\omega_0\tau_{\text{pt}}\varphi_{\text{pt}}^{\pm} = \mp 0.15$ due to the photothermal force while the contribution of the radiation force of $Q_0\omega_0\tau_{\text{rad}}\varphi_{\text{rad}}^{\pm} = \pm 3.5 \times 10^{-9}$ is negligible. From this analysis we find that under realistic conditions of NC-AFM operation, the photon pressure yields a minute 3.5 ppm shift in the resonance frequency and change in spring constant of the force detection system while the Q -factor exhibits a significant 15% change due to the photothermal force.

For a practical exploitation of the optomechanical coupling to improve the performance of a dynamic force microscope based on interferometric detection, we can take advantage of the orders of magnitude between the weighting factors $\omega_0\tau$ for photothermal and radiation based effects. The basic idea is to use the interferometer cavity for optical Q -control in analogy to electronic devices designed for enhancing the Q -factor for dynamic force microscopy in low- Q environments.²³ When operating the interferometer on a positive slope, this could be used to enhance the sensitivity in NC-AFM measurements limited by thermal noise⁴ as the detection limit scales with $Q^{-1/2}$. Note, however, that in a high- Q environment this is a critical procedure strictly restricted to the regime where $1 + Q_0\omega_0\tau_{\text{pt}}\varphi_{\text{pt}}^+(P) > 0$. As evident from Eq. (2), increasing P beyond this limit yields a negative damping inevitably driving the system into the regime of uncontrolled self-oscillation.²⁴ To be far away from such conditions of instability is the reason for using a cantilever with a relatively low Q -factor¹⁵ for this study aiming at the exploration of optomechanical interactions at positions of positive and negative slope.

While the enhancement of the Q -factor is desirable for NC-AFM measurements in a low- Q environment like water,²⁵ for measurements in the UHV, it may be desirable to use optical Q -control to reduce the Q -factor. For high performance cantilevers, the product of $Q_0\omega_0$ may readily exceed 10^9 where the extreme narrow resonance peaks associated

with such cantilevers are a severe challenge for stable operation of electronics used to maintain a constant cantilever oscillation amplitude and to detect the resonance frequency shift. In this case, one can operate the interferometer on a negative slope and limit the effective Q -factor to a value adjusted by the light power in the cavity.

In summary, we demonstrate that it is possible to quantify the optomechanical forces acting on the interferometric detection system of a dynamic force microscope at room temperature. By an adjustment of these forces one can enhance or reduce the Q -factor of the force detection system as appropriate for a specific measurement. This is a new degree of freedom for the optimization of NC-AFM measurements available for interferometer based detection systems at minimum cost.

- ¹J. Hough, S. Rowan, and B. S. Sathyaprakash, *J. Phys. B* **38**, S497 (2005).
- ²H. O. Özer, S. J. O'Brien, and J. B. Pethica, *Appl. Phys. Lett.* **90**, 133110 (2007).
- ³D. Rugar, H. J. Mamin, R. Erlandsson, J. E. Stern, and B. D. Terris, *Rev. Sci. Instrum.* **59**, 2337 (1988).
- ⁴T. R. Albrecht, P. Grütter, D. Horne, and D. Rugar, *J. Appl. Phys.* **69**, 668 (1991).
- ⁵C. Metzger and K. Karrai, *Nature (London)* **432**, 1002 (2004).
- ⁶F. Marquardt, J. G. E. Harris, and S. M. Girvin, *Phys. Rev. Lett.* **96**, 103901 (2006).
- ⁷T. J. Kippenberg and K. J. Vahala, *Science* **321**, 1172 (2008).
- ⁸H. Hölscher, P. Milde, U. Zerweck, L. M. Eng, and R. Hoffmann, *Appl. Phys. Lett.* **94**, 223514 (2009).
- ⁹M. Vogel, C. Mooser, K. Karrai, and R. J. Warburton, *Appl. Phys. Lett.* **83**, 1337 (2003).
- ¹⁰C. Metzger, I. Favero, A. Ortlieb, and K. Karrai, *Phys. Rev. B* **78**, 035309 (2008).
- ¹¹A. Schwarz, U. D. Schwarz, S. Langkat, H. Hölscher, W. Allers, and R. Wiesendanger, *Appl. Surf. Sci.* **188**, 245 (2002).
- ¹²J. P. Cleveland, S. Manne, D. Bocek, and P. K. Hansma, *Rev. Sci. Instrum.* **64**, 403 (1993).
- ¹³E. M. Ceresa and F. Garbassi, *Mater. Chem. Phys.* **9**, 371 (1983).
- ¹⁴S. M. Sze, *Physics of Semiconductor Devices* (Wiley, New York, 1981).
- ¹⁵J. Lübke, L. Tröger, S. Torbrügge, R. Bechstein, C. Richter, A. Kühnle, and M. Reichling, *Meas. Sci. Technol.* **21**, 125501 (2010).
- ¹⁶D. Rugar, H. J. Mamin, and P. Guethner, *Appl. Phys. Lett.* **55**, 2588 (1989).
- ¹⁷A. D. Drake and D. C. Leiner, *Rev. Sci. Instrum.* **55**, 162 (1984).
- ¹⁸B. S. Sheard, M. B. Gray, C. M. Mow-Lowry, D. E. McClelland, and S. E. Whitcomb, *Phys. Rev. A* **69**, 051801 (2004).
- ¹⁹J. R. Chelikowsky and M. L. Cohen, *Phys. Rev. B* **14**, 556 (1976).
- ²⁰J. R. Chelikowsky and M. L. Cohen, *Phys. Rev. B* **30**, 4828 (1984).
- ²¹I. Favero and K. Karrai, *New J. Phys.* **10**, 095006 (2008).
- ²²H. R. Shanks, P. D. Maycock, P. H. Sidles, and G. C. Danielson, *Phys. Rev.* **130**, 1743 (1963).
- ²³H. Hölscher, D. Ebeling, and U. D. Schwarz, *J. Appl. Phys.* **99**, 084311 (2006).
- ²⁴O. Arcizet, P. F. Cohadon, T. Briant, M. Pinard, and A. Heidmann, *Nature (London)* **444**, 71 (2006).
- ²⁵S. Rode, N. Oyabu, K. Kobayashi, H. Yamada, and A. Kühnle, *Langmuir* **25**, 2850 (2009).